Electronic Supplementary Material (ESI) for Chemical Communications.

Crystal engineering of zwitterionic drug to neutral cocrystal: a general solution for floxacins

Anilkumar Gunnam,[a] Kuthuru Suresh,[a] Ramesh Ganduri,[b] and Ashwini Nangia*[a,c]

E-mail: ashwini.nangia@gmail.com; ak.nangia@ncl.res.in

[a] School of Chemistry, University of Hyderabad, Central University P.O., Prof. C. R. Rao Road, Hyderabad 500 046, India

[b] Solid State and Structural Chemistry Unit, Indian Institute of Science, Bengaluru 560 012, India

[c] CSIR-National Chemical Laboratory, Dr. Homi Bhabha Road, Pune 411 008, India

Table S1 CCDC Refcodes of zwitterion quinolone compounds.

SESZEW	ROMDUT	COVPIN02	CONYOU
QEDPUM	PUZGAT01	COVPIN01	CONYIO
ENODOB	PUZGAT	COVPIN	UHITUB01
YEPMEJ	NIWQIU	COJZIV	UHITUB
XICPEG	HOXMUD	COQWOU02	LATPON
XAYGEJ01	ENODUH01	COQWOU01	KEXGAX
XAYGEJ	ENODUH	COQWOU	VETVUM

Table S2 Crystallographic parameters of SPX cocrystals.

	SPX–MBZ(1:1)	**SPX–EBZ(1:1)**	**SPX–PBZ(1:1)**	**SPX–IBZ(1:1)**
Emp. form.	$C_{27}H_{30}F_2N_4O_6$	$C_{28}H_{32}F_2N_4O_6$	$C_{29}H_{34}F_2N_4O_6$	$C_{30}H_{36}F_2N_4O_6$
Form. wt	544.55	558.58	572.60	586.63
Cryst. syst.	Triclinic	Triclinic	Triclinic	Triclinic
Sp. Gr.	*P*-1	*P*-1	*P*-1	*P*-1
T (K)	298(2)	298(2)	298(2)	298(2)
a (Å)	9.423(5)	9.5457(5)	7.9588(4)	9.5693(7)
b (Å)	12.742(7)	12.8769(6)	10.3333(5)	9.7134(7)
c (Å)	12.890(7)	13.3380(7)	17.8484(9)	17.7964(12)
α (°)	62.717(9)	62.8916(14)	80.749(4)	74.767(3)
β (°)	70.160(9)	71.3599(16)	87.489(4)	76.025(3)
γ (°)	76.407(10)	77.1301(16)	72.019(5)	69.597(3)
Z	2	2	2	2
V (Å^3)	1288.0(12)	1377.05(12)	1377.99(13)	1475.24(18)
Rflns. Collect.	5101	6391	8441	5270
Unique. Rflns.	4973	6368	7354	5258
Obsd. Rflns.	2756	4567	4637	2755
Parameters	450	377	373	391
R_1	0.0605	0.0498	0.0753	0.0638

wR_2	0.1538	0.1729	0.2210	0.1517
GOF	0.908	1.106	1.087	1.030
Diffractometer	Bruker CCD area detector	Bruker CCD area detector	Oxford Xcalibur Gemini	Bruker CCD area detector

Table S3 Hydrogen bonding in SPX cocrystals and salts (N–H, O–H, and C–H distances are neutron-normalized).

D–H···A	D···A (Å)	H···A (Å)	D–H···A (°)	symmetry code
SPX–MBZ				
O2–H2A···O1	2.502(3)	1.54	154	---[a]
N2–H2B···O3	3.081(4)	2.28	160	1+x,y,z
N2–H2C···O1	2.673(4)	2.00	132	---[a]
N4–H4A···O2	3.086(4)	2.28	171	1+x,-1+y,z
O6–H6A···N4	2.711(4)	1.84	170	-1+x,y,z
C9–H9···F2	3.307(4)	2.37	160	-1+x,y,z
C14–H14A···O3	3.308(4)	2.57	132	-x,2-y,-z
SPX–EPZ				
O2–H2A···O1	2.504(2)	1.72	154	---[a]
N2–H2B···O3	3.244(3)	2.46	156	1+x,y,z
N2–H2C···O1	2.664(3)	2.06	128	---[a]
N4–H4A···O2	3.165(2)	2.27	167	1+x,-1+y,z
O6–H6A···N4	2.687(3)	1.87	163	2-x,-y,1-z
C14–H14A···O3	3.277(3)	2.54	131	-x,1-y,1-z
C28–H28A···O3	3.471(4)	2.50	170	-x,1-y,1-z
SPX–PBZ				
O2–H2A···O1	2.532(3)	1.78	152	---[a]
N2–H2B···O1	2.638(3)	1.99	131	---[a]
N2–H2C···O6	3.162(3)	2.40	148	1-x,1-y,-z
N4–H4A···O4	3.045(3)	2.16	172	-1+x,y,z
O6–H6A···N4	2.621(3)	1.82	166	1-x,-y,-z
C14–H14A···O3	3.456(3)	2.50	169	1-x,1-y,1-z
C25–H25···O3	3.327(3)	2.40	177	x,y,-1+z
SPX-IBZ				
O2–H2A···O1	2.535(4)	1.59	156	---[a]
N2–H2B···O3	3.107(4)	2.28	163	-1+x,y,z
N4–H4A···O4	3.042(4)	2.20	162	1+x,y,z
O6–H6A···N4	2.708(4)	1.92	161	-x,-y,1-z
C9–H9···F2	3.415(5)	2.54	157	1+x,y,z
C13–H13A···O3	3.395(5)	2.49	154	2-x,2-y,-z
N2–H2C···O1	2.659(4)	2.02	130	---[a]

[a]intramolecular hydrogen bond

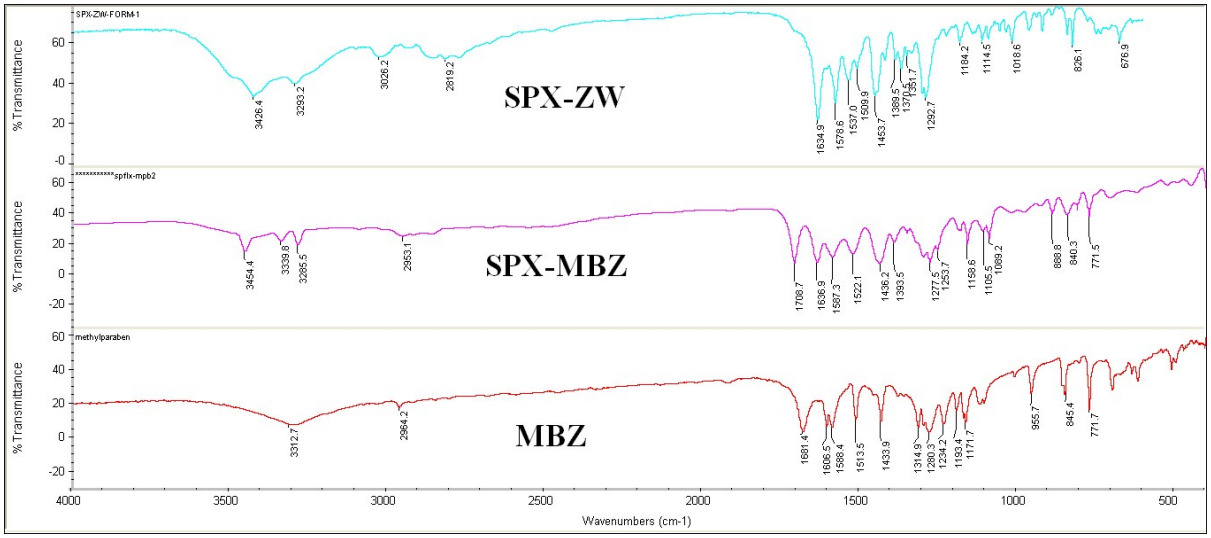

FigureS1a Overlay of SPX-MBZcocrystal IR spectra with its starting components.

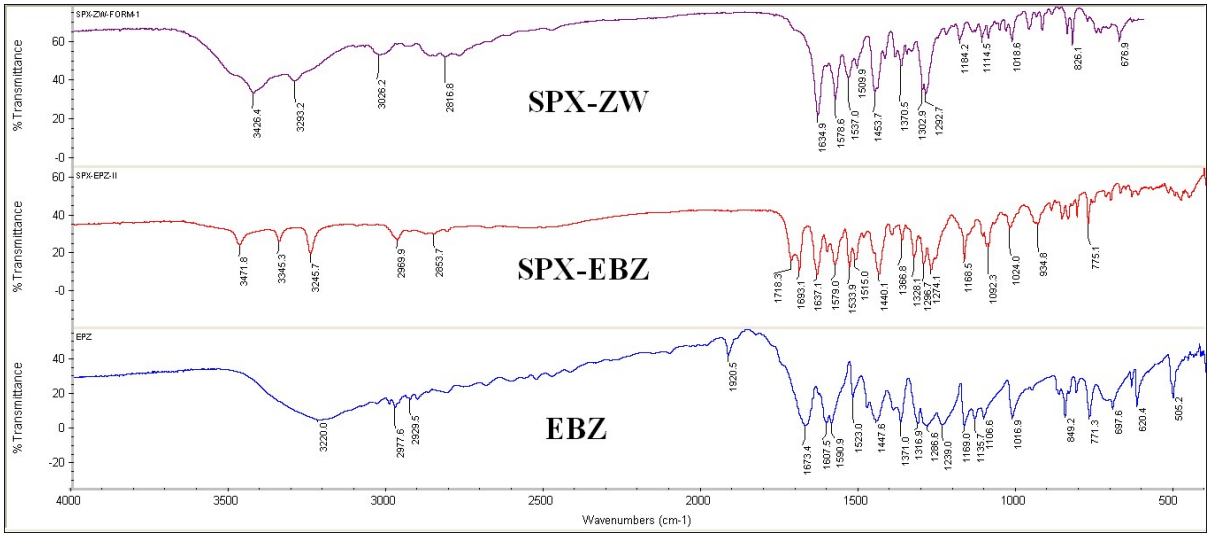

FigureS1b Overlay of SPX-EBZcocrystal IR spectra with its starting components.

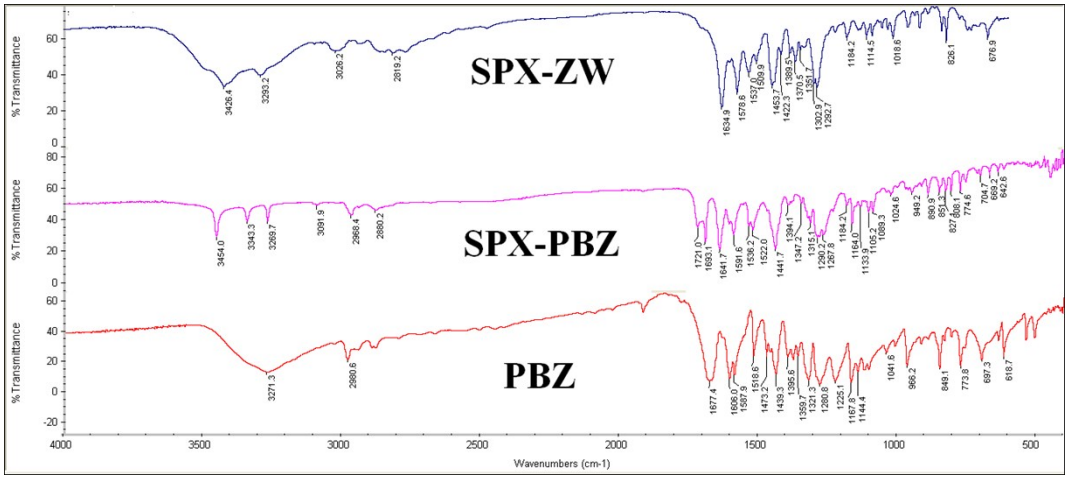

FigureS1c Overlay of SPX-PBZcocrystal IR spectra with its starting components.

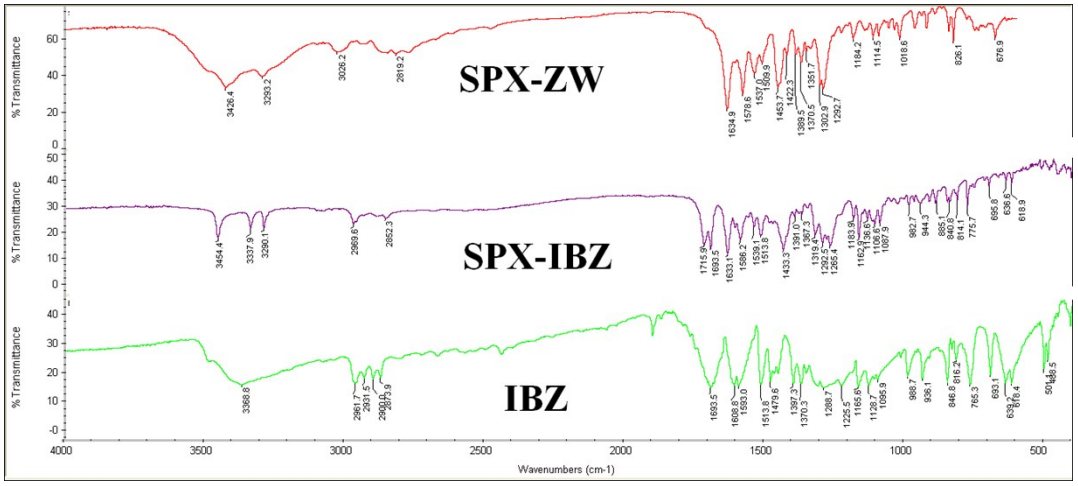

FigureS1d Overlay of SPX-IBZcocrystal IR spectra with its starting components.

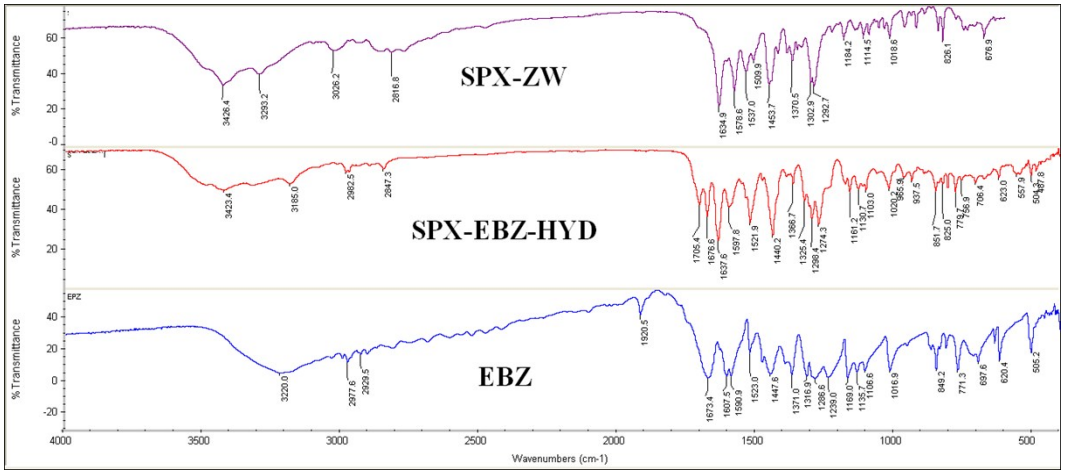

FigureS1e Overlay of SPX-EBZ-HYDcocrystal IR spectra with its starting components.

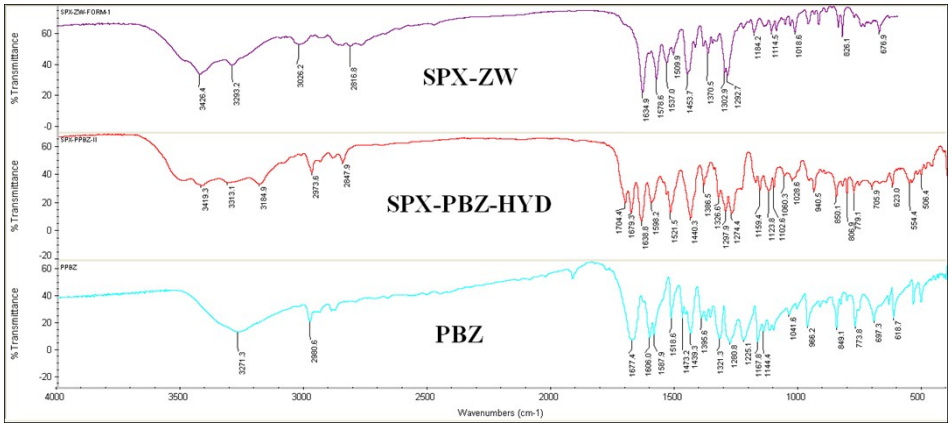

Figure S1f Overlay of SPX-PBZ-HYDcocrystal IR spectra with its starting components.

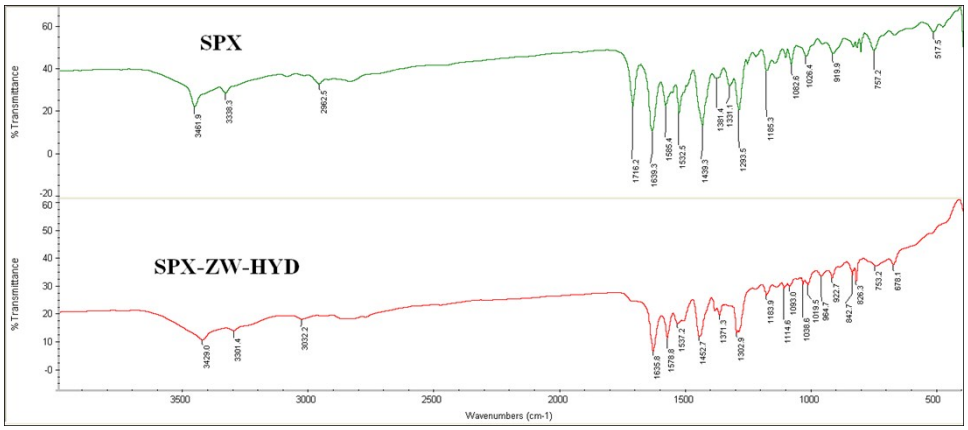

Figure S1 g Overlay of SPX neutral and zwitterion forms IR spectra.

Figure S1a-gFT-IR spectra of SPX solid forms (sample prepared as KBr pellet).

Table S4 FT-IR stretching frequencies of SPX and parabencoformer in crystalline form.

	OH/NH Stretching (cm^{-1})	OH/NH Stretching (cm^{-1})	C=O Stretching of -COOH of SPX and COOR in coformer (cm^{-1})	C=O Stretching ofpyridinone (cm^{-1})
SPX	--	3461,3338	1716	1639
SPX-ZW	--	3429,3301	--	1635
MBZ	3312	--	1681	--
SPX-MBZ	3285	3454,3339	1708	1636
EBZ	3220	--	1673	--
SPX-EBZ	3247	3466,3343	1717, 1691	1637
SPX-EBZ-HYD	3185	3423	1705, 1676	1637
PBZ	3271	--	1677	--
SPX-PBZ	3184	3415	1704, 1679	1638
SPX-PBZ-HYD	3184	3419, 3313	1704, 1679	1638
IBZ	3368	--	1693	--
SPX-IBZ	3290	3454, 3337	1715, 1693	1633

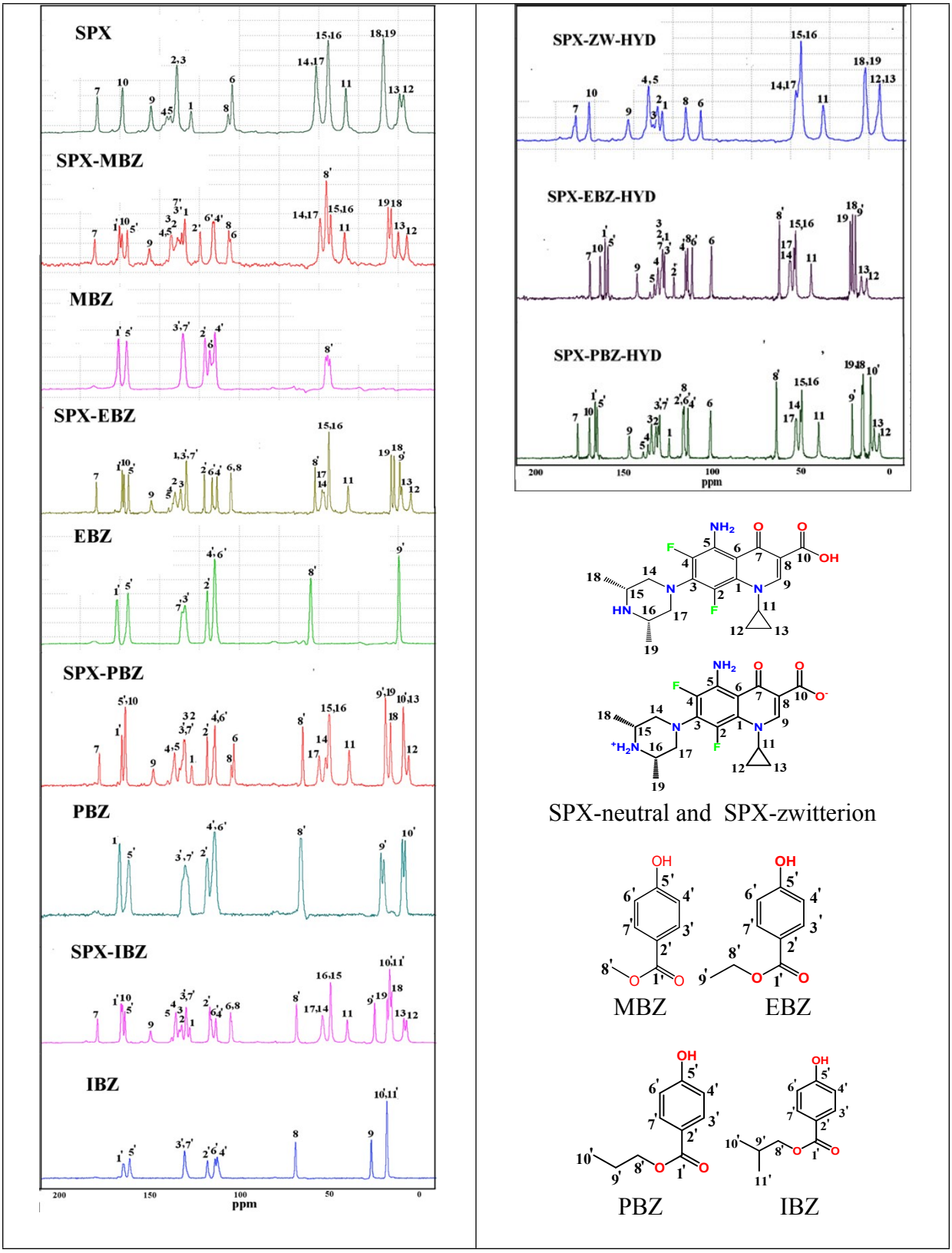

Figure S2 ss-NMR comparison of SPX cocrystals with SPX neutral, zwitterion and coformer peaks.

Table S5 ss-NMR peaks comparison of SPX cocrystals with SPX neutral, zwitterion and coformer values (atom numbering as shown in Figure S2).

S.No.	SPX	SPX-ZW-HYD	SPX-MBZ	SPX-EBZ	SPX-PBZ	SPX-IBZ	SPX-EBZ-HYD	SPX-PBZ-HYD
1	126.6	127.9	129.8	129.1	126.2	127.5	129.9	124.2
2	134.3	130.5	133.0	132.2	130.0	131.9	131.0	131.6
3	134.3	133.2	133.8	132.2	130.5	133.3	131.0	134.1
4	139.8	135.6	137.2	135.3	135.7	135.1	133.8	136.2
5	137.9	135.6	137.2	135.3	135.7	135.1	136.1	138.8
6	103.7	106.2	104.6	104.4	102.8	104.2	100.9	100.8
7	178.6	176.5	179.7	178.9	177.4	178.7	175.7	175.8
8	**106.9**	**114.6**	**105.6**	**104.4**	**104.3**	**104.9**	**115.7**	**115.8**
9	148.7	147.0	149.5	148.5	147.5	149.2	146.7	146.7
10	**164.5**	**169.0**	**164.6**	**163.5**	**163.1**	**164.8**	**169.4**	**169.1**
11	40.9	37.5	41.5	39.5	38.9	40.1	39.6	39.8
12	8.9	5.7	7.1	4.8	5.9	7.2	5.4	5.7
13	11.0	5.7	11.8	9.9	8.9	8.7	8.7	8.4
14	57.3	52.7	55.0	52.8	51.9	53.9	52.3	52.4
15	50.7	49.9	49.1	50.2	50.0	49.3	49.2	49.3
16	50.7	49.9	49.1	50.2	50.0	49.3	50.1	50.1
17	57.3	52.7	55.0	53.9	55.6	53.9	52.9	52.7
18	20.0	13.7	15.7	14.0	15.9	15.5	14.3	14.7
19	20.0	13.7	17.4	15.7	18.8	18.0	15.6	15.3
20(1')			166.0	164.6	165.0	165.5	166.4	165.9
21(2')			121.2	119.1	117.6	116.3	124.0	115.8
22(3')			131.5	129.1	130.0	129.5	129.9	129.6
23(4')			113.7	112.1	113.3	113.0	116.9	113.6
24(5')			161.7	161.0	163.1	163.4	164.6	164.8
25(6')			114.3	114.8	114.0	115.6	112.8	116.3
26(7')			131.5	129.1	130.5	129.5	131.0	130.3
27(8')			51.6	57.9	64.9	68.3	59.3	63.6
28(9')				11.0	18.8	25.0	12.4	20.8
29(10')					8.9	16.6		10.5
30(11')						16.6		
			MBZ	**EBZ**	**PBZ**	**IBZ**		
1'			166.8	167.5	166.2	164.2		
2'			118.7	117.6	117.6	117.5		
3'			131.1	129.9	129.9	130.2		
4'			113.4	113.4	113.5	112.1		
5'			162.3	161.4	161.2	160.7		
6'			116.2	113.4	113.5	113.3		
7'			131.1	131.4	129.9	130.2		
8'			51	60.3	65.5	68.6		
9'				11.5	21.3	26.5		
10'					9.5	17.9		
11'						17.9		

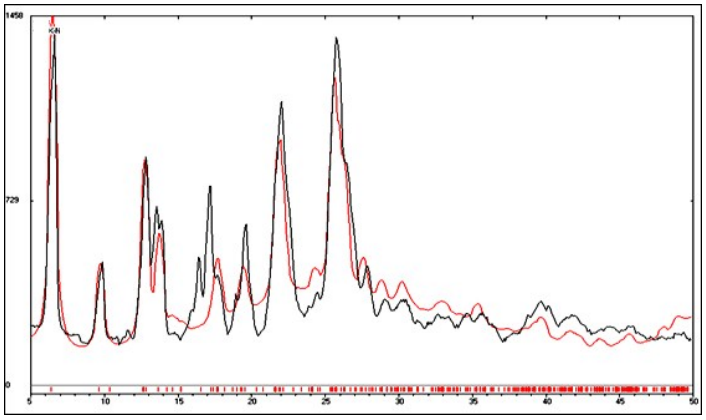

Figure S3a Overlay of the experimental SPX-neutral PXRD pattern (black) and the calculated diffraction lines from the single crystal structure (red).

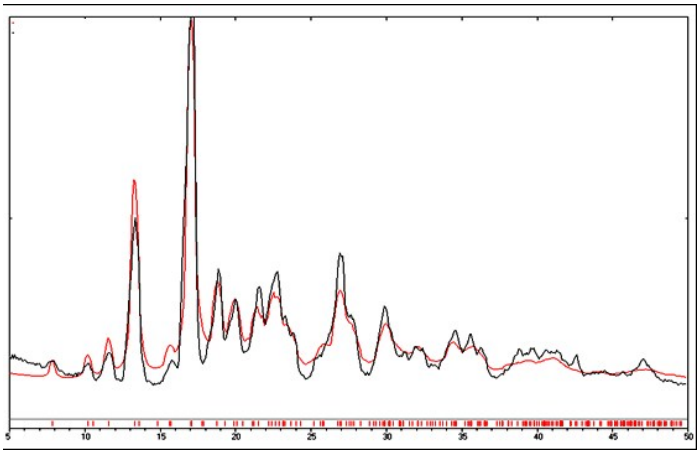

Figure S3b Overlay of the experimental zwitterion form II, PXRD pattern (black) and the calculated diffraction lines from the single crystal structure (red).

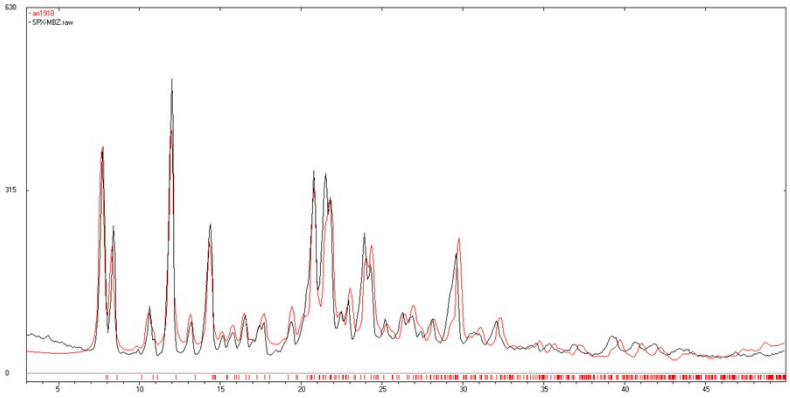

Figure S3c Overlay of the experimental SPX-MBZ, PXRD pattern (black) and the calculated diffraction linesfrom the single crystal structure (red).

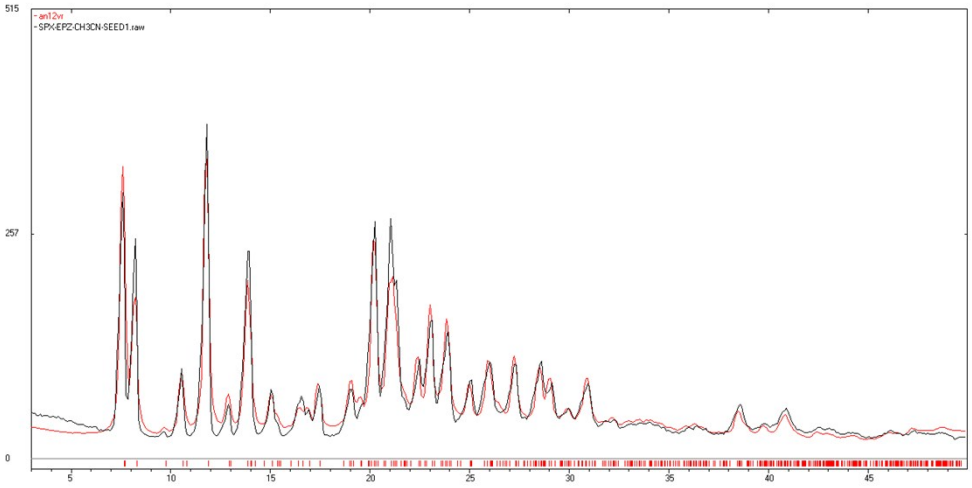

Figure S3d Overlay of the experimental SPX-EBZ, PXRD pattern (black) and the calculated diffraction linesfrom the single crystal structure (red).

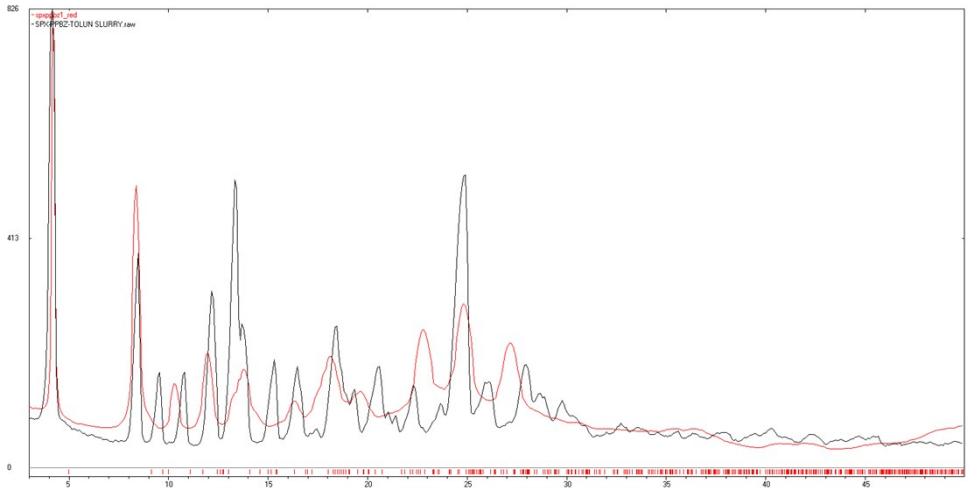

Figure S3e Overlay of the experimental SPX-PBZ, PXRD pattern (black) and the calculated diffraction lines from the single crystal structure (red).

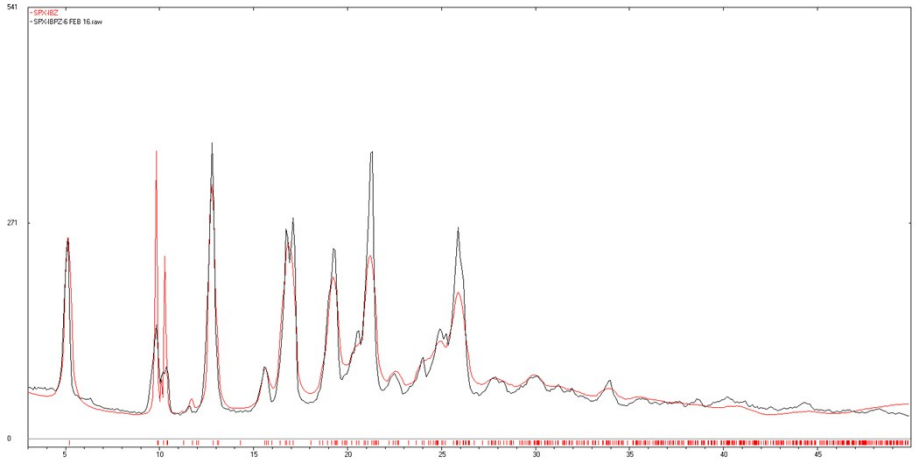

Figure S3f Overlay of the experimental SPX-IBZ, PXRD pattern (black) and the calculated diffraction lines from the single crystal structure (red).

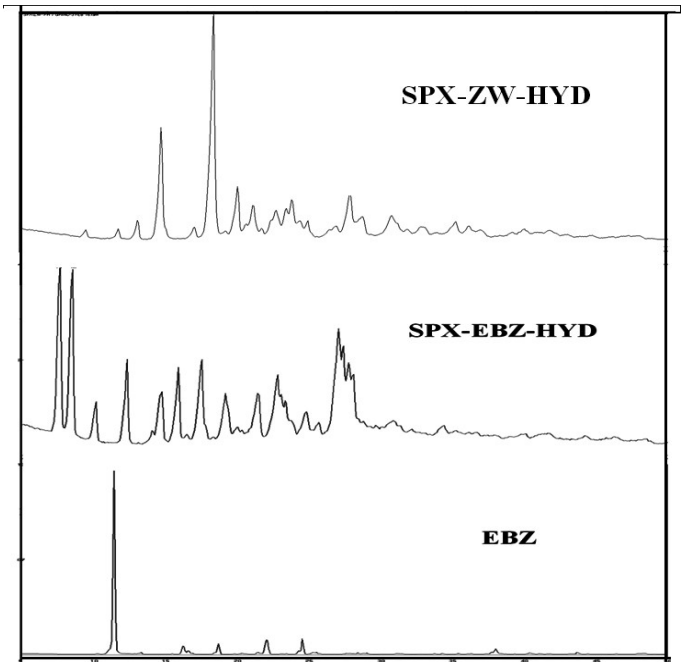

Figure S3g Experimental PXRD plots of SPX-ZW-HYD, and EBZ to compare 2θ values in the new crystalline phase of SPX-EBZ-HYD.

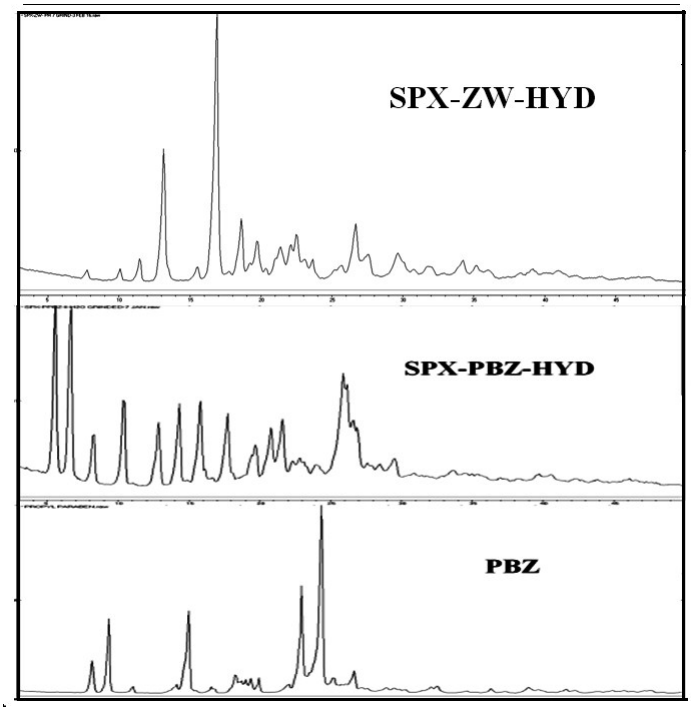

Figure S3h Experimental PXRD plots of SPX-ZW-HYD and EBZ to compare 2θ values in the new crystalline phase SPX-PBZ-HYD.

Figure S3a-h Powder XRD comparison of SPX and product crystal forms.

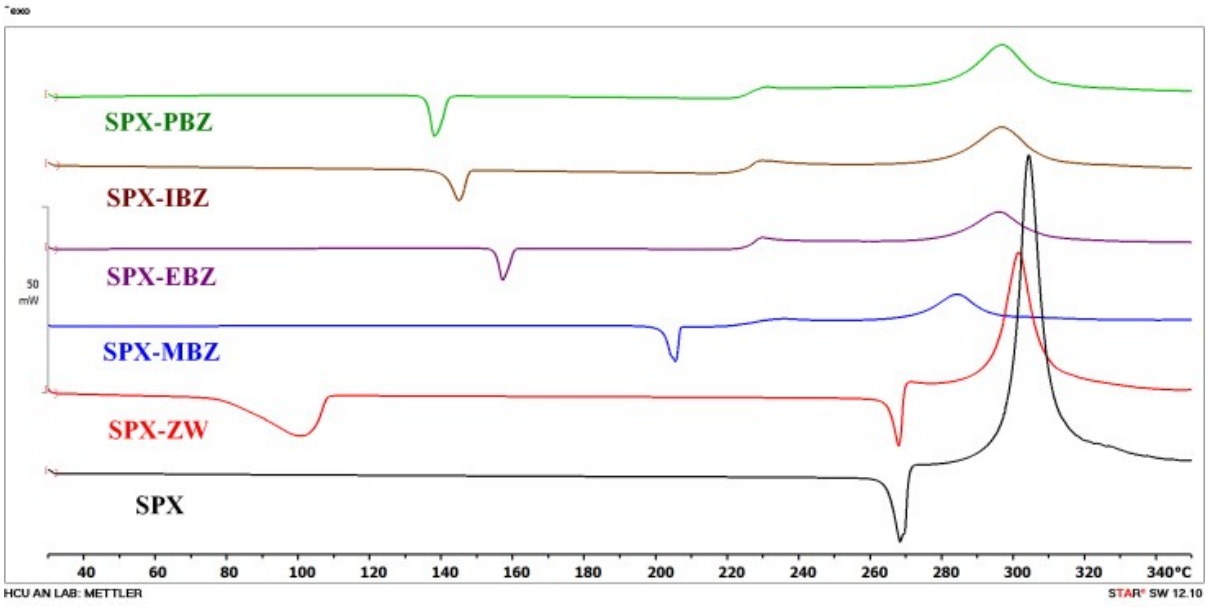

Figure S4 DSC thermogram of SPX neutral, zwitterion and cocrystals.

Table S6 Melting point of SPX, coformers and cocrystals.

Drug/ conformer	Melting point (°C)	cocrystal	Melting point of cocrystal (°C)
SPX neutral	264-267	-	-
SPX zwitterion	264-267	-	-
MBZ	126-128	SPX-MBZ	201-205
EBZ	115-118	SPX-EBZ	154-157
	-	SPX-EBZ-HYD	152-155
PBZ	96-99	SPX-PBZ	135-134
	-	SPX-PBZ-HYD	132-134
IBZ	75-78	SPX-IBZ	140-144

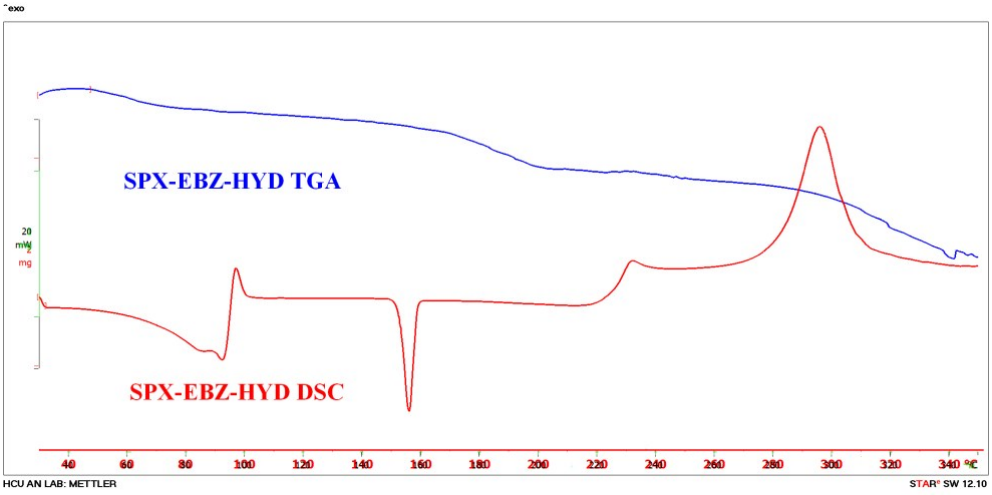

Figure S5 DSC (red) and TGA (blue) of SPX-EBZ-HYD. The weight loss in TGA is consistent with three molecules of H_2O in the cocrystal hydrate structure.

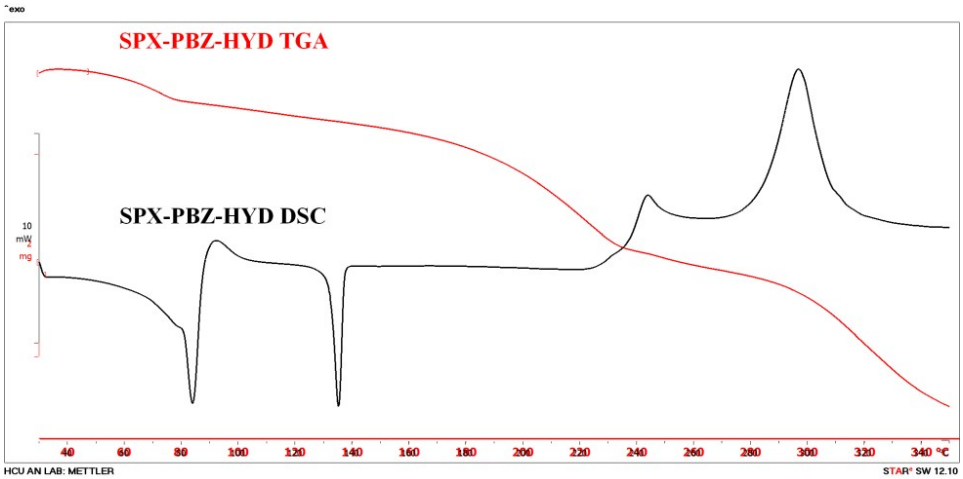

Figure S6 DSC (red) and TGA (blue) of SPX-EBZ-HYD. The weight loss in TGA is consistent with three molecules of H_2O in the cocrystal hydrate structure.

The TGA analysis of SPX-EBZ-HYD showed a weight loss of 9.21% corresponds to water loss of 0.188 mg from initial weight of 2.05 mg indicates the presence of three water molecules in SPX-EBZ-HYD, i.e. SPX-EBZ-HYD (1:1:3). SPX-PBZ-HYD showed a weight loss of 9.31% corresponding to water loss of 0.354 mg from initial weight of 3.80 mg indicates presence of three water molecules in SPX-PBZ-HYD, i.e. SPX-PBZ-HYD (1:1:3).

Table S7 Weight loss in TGA of SPX cocrystals Hydrates

Compound	Initial weight (in mg)	% Loss of water Obs. (calc. by trihydrate)	Weight loss at 60 – 100°C (in mg)	Equivalents of water molecules by TGA
SPX-EBZ-HYD	2.05	9.21 (8.82)	0.188	3.13
SPX-PBZ-HYD	3.80	9.31 (8.62)	0.354	3.24

M.W.: SPX-EBZ-3HYD = 558+54 = 612; SPX-PBZ-3HYD = 572+54 = 626

Table S7 Intrinsic dissolution rates of SPX neutral, zwitterionic forms, cocrystals and salts.

Compound	Coformer Water Solubility (mg/mL)	Molar Extinction coefficient (μM^{-1} cm^{-1})	Intrinsic dissolution rate, IDR (mg/cm^2)/min	Equilibrium Solubility (mg/L)
SPX	0.11	0.008	0.042(x0.91)	
SPX-ZW	0.11	0.008	0.046 (x1. 09)	184.6
SPX-MBZ	2.50	0.008	0.054 (x1.17)	248.68(x1.34)
SPX-EBZ	0.88	0.008	0.063(x1.36)	-
SPX-EBZ-HYD	-	0.008	0.051(x1.10)	598.42(x3.24)
SPX-PBZ	0.50	0.008	0.086(x1.86)	-
SPX-PBZ-HYD	-	0.007	0.069(x1.50)	723.15(x3.91)
SPX-IBZ	0.22	0.008	0.046(x1.00)	259.97(x1.40)

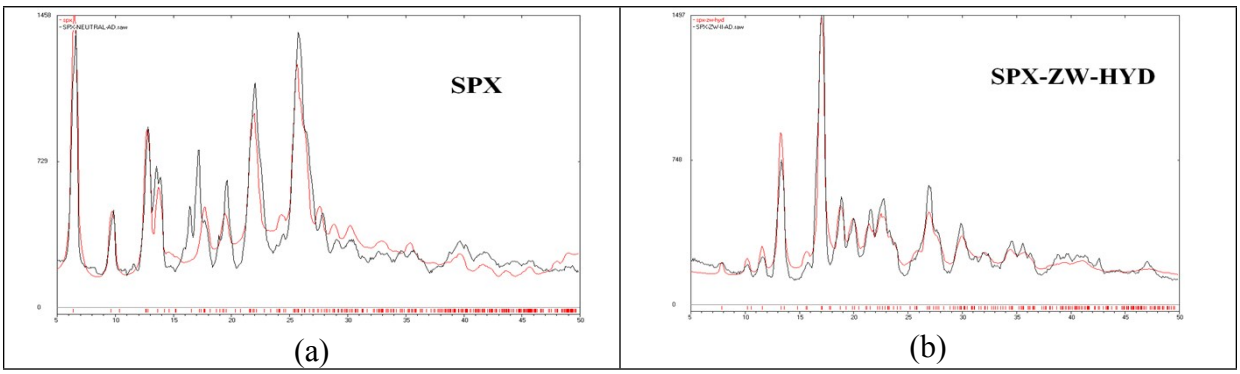

(a) (b)

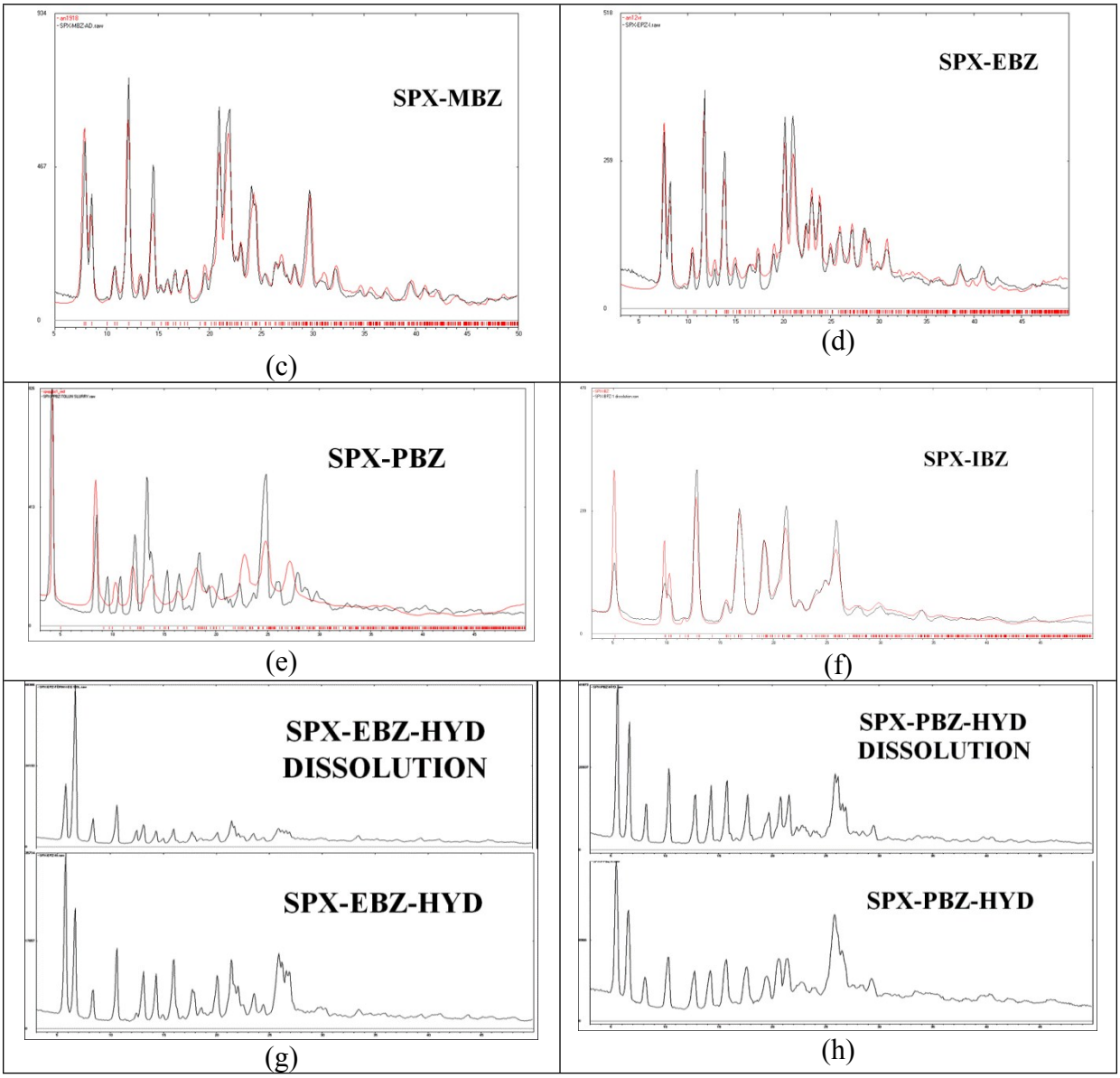

Figure S7a-h PXRD of solids SPX neutral, zwitterion and cocrystals at the end of dissolution experiment (4 h, black) matches with the calculated XRD pattern of the anhydrate forms, and cocrystal hydrates match with the starting experimental PXRD, indicating phase stability of these solids.

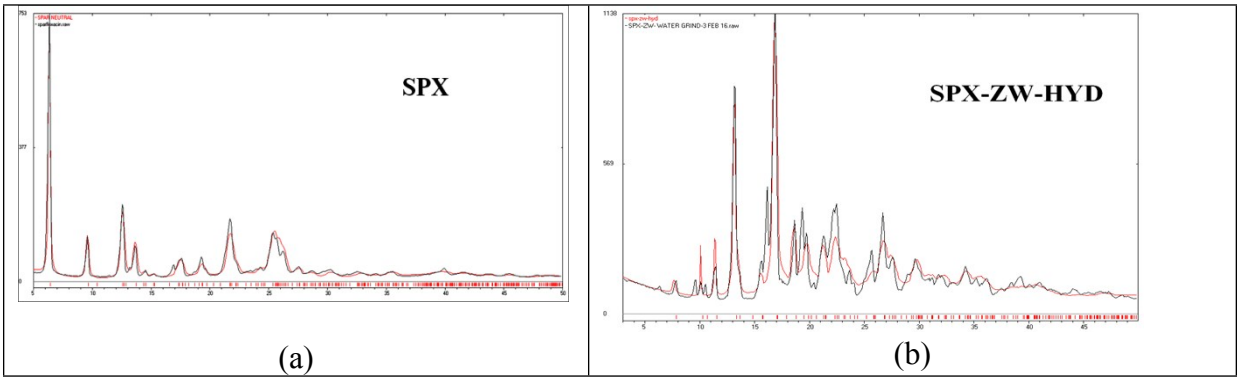

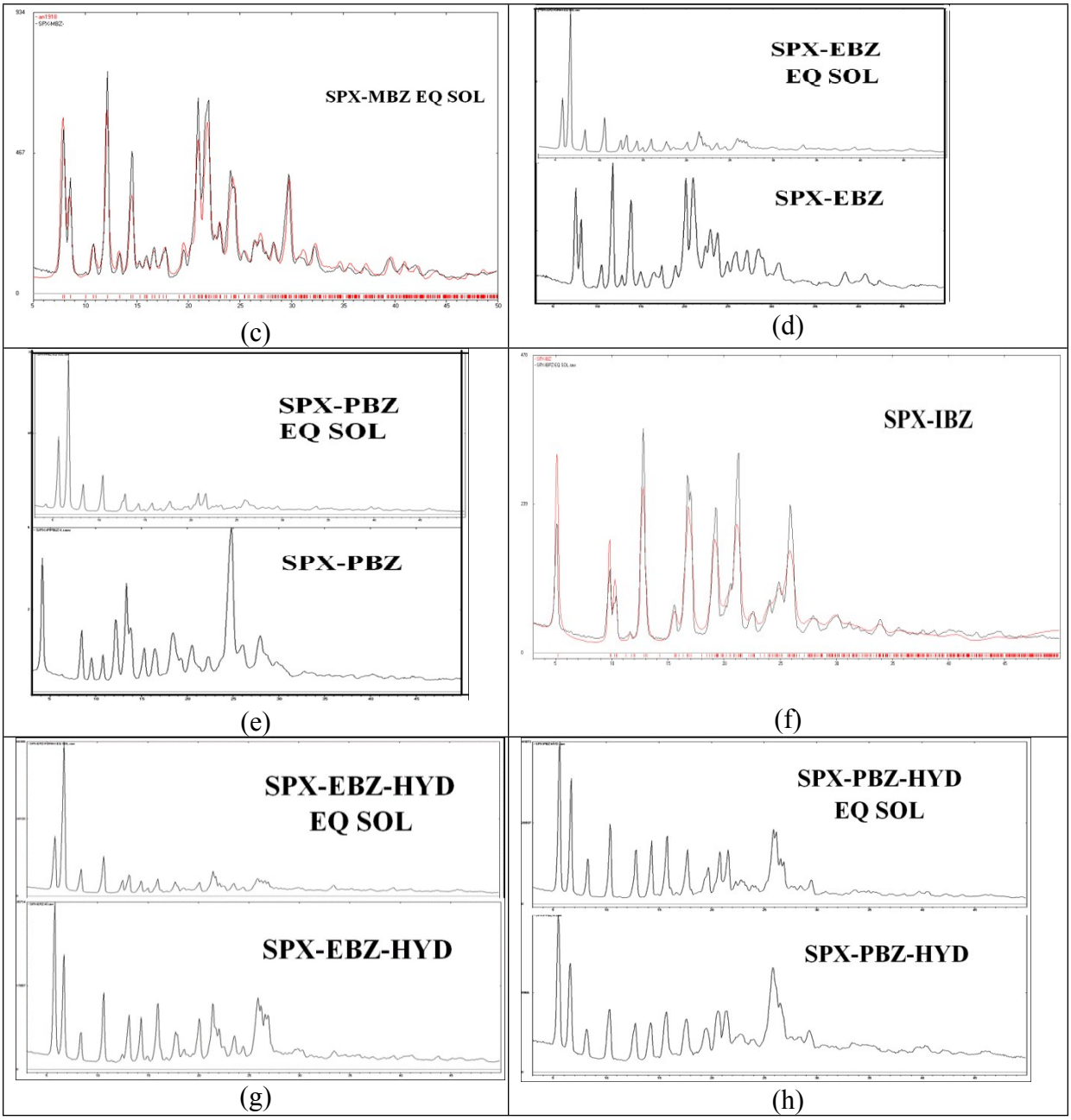

Figure S8a-h PXRD of SPX-ZW, SPX-MBZ, SPX-IBZ, SPX-EBZ-HYD and SPX-PBZ-HYD at the end of equilibrium solubility measurement (24 h, black) matches with the calculated PXRD pattern or starting experimental PXRD pattern, indicating extended phase stability of the solids. SPX neutral form, SPX-EBZ and SPX-PBZ converted to SPX zwitterion hydrate.

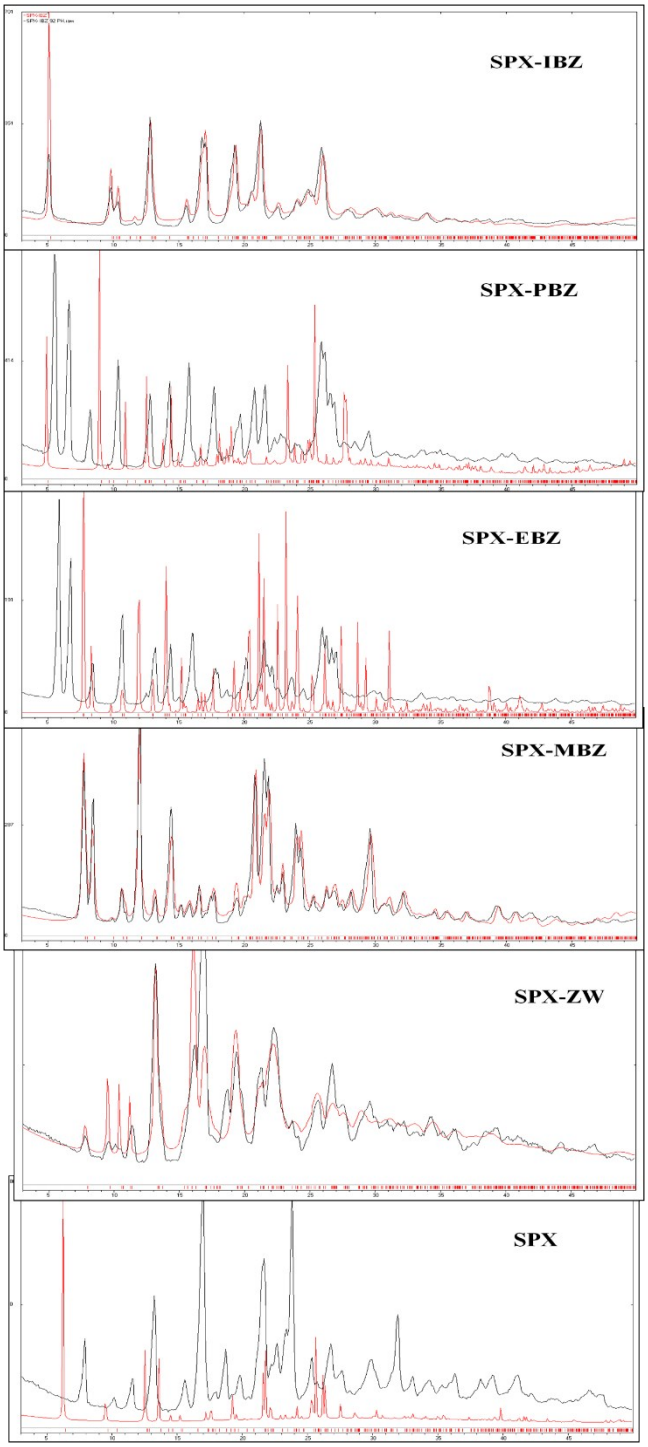

Figure S9 PXRD of SPX-ZW, SPX-MBZ and SPX-IBZ at the end of phase stability experiment in water (24 h, black) matches with the calculated PXRD pattern indicating extended phase stability of the solids. SPX neutral form, SPX-EBZ and SPX-PBZ converted to the zwitterion hydrate. The products do not match with starting material PXRD pattern but with the hydrate PXRD lines.

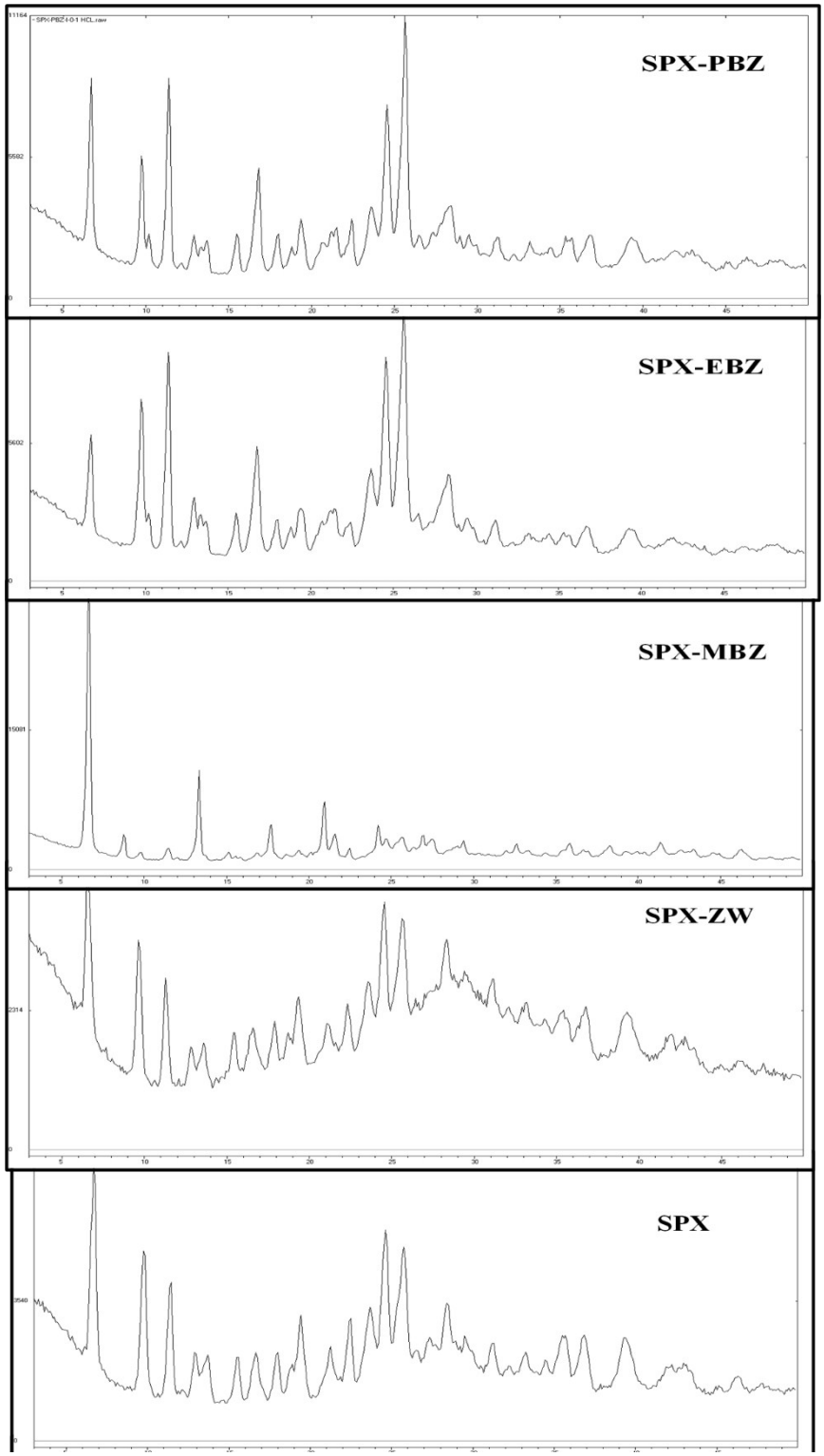

Figure 10 PXRD of SPX, SPX-ZW, SPX-MBZ, SPX-IBZ, SPX-EBZ and SPX-PBZ at the end of phase stability experiment in pH 1.2 (24 h, black) medium. All the solids are converted to a new phase in 0.1 N HCl which may be the hydrochloride salt.

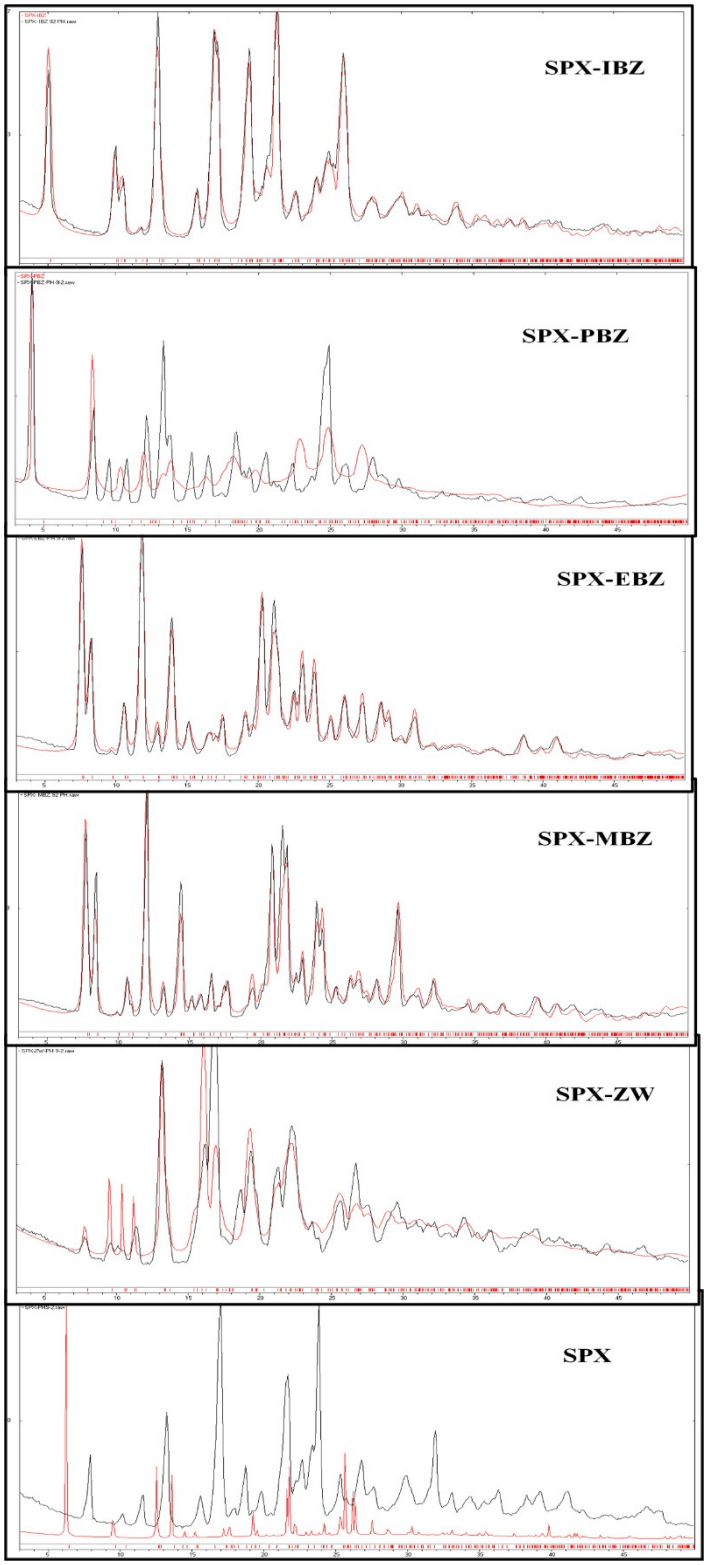

Figure 11 PXRD of SPX, SPX-ZW, SPX-MBZ, SPX-IBZ, SPX-EBZ and SPX-PBZ at the end of phase stability experiment in pH 9.2 (24 h, black) matches with the calculated PXRD pattern indicating extended phase stability of these solids. SPX neutral form converted to its zwitterion hydrate.

Figure S12a-h DVS plots of SPX solids neutral, zwitterion, cocrystals and cocrystal hydrates to show the water uptake at 90% RH conditions.

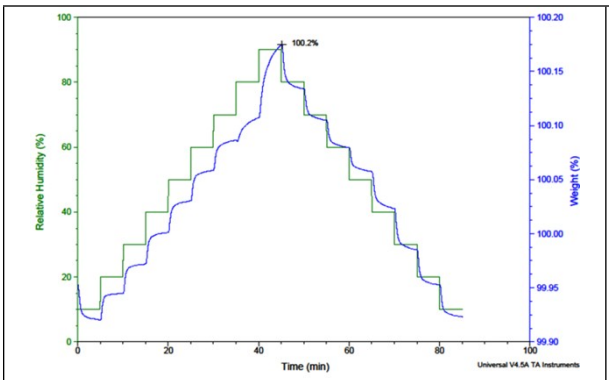

(a) SPX (absorbed water 0.2%)

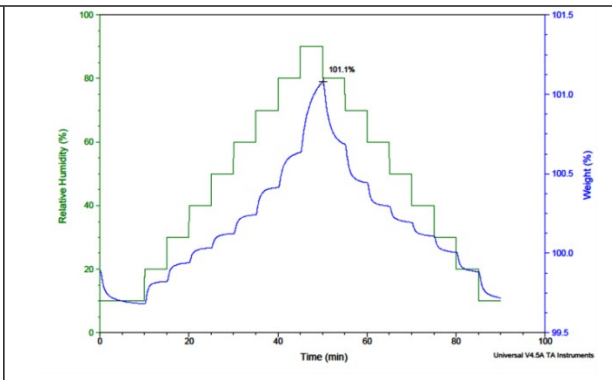

(b) SPX-ZW-HYD (absorbed water 1.1%)

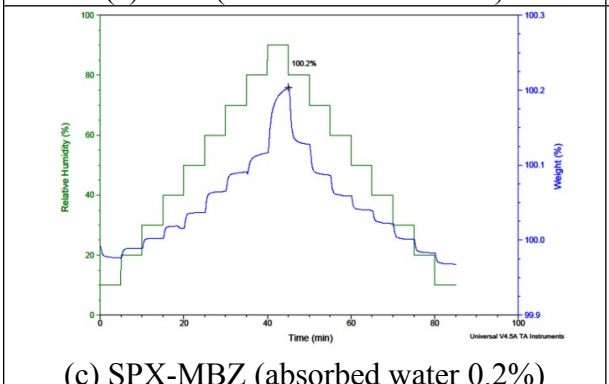

(c) SPX-MBZ (absorbed water 0.2%)

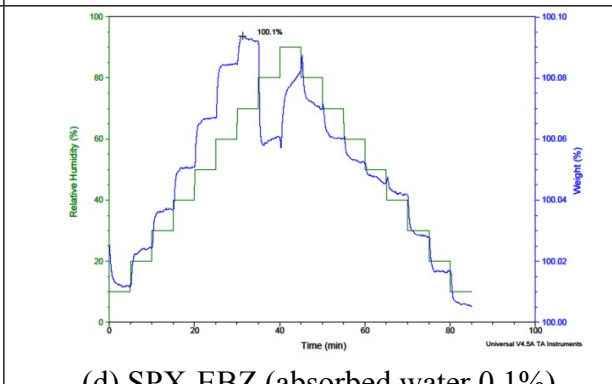

(d) SPX-EBZ (absorbed water 0.1%)

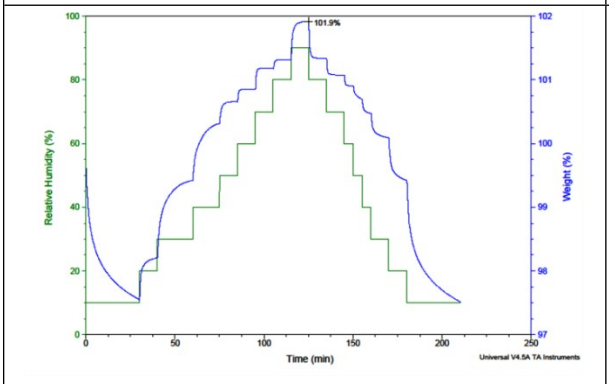

(e) SPX-EBZ-HYD (absorbed water 1.9%)

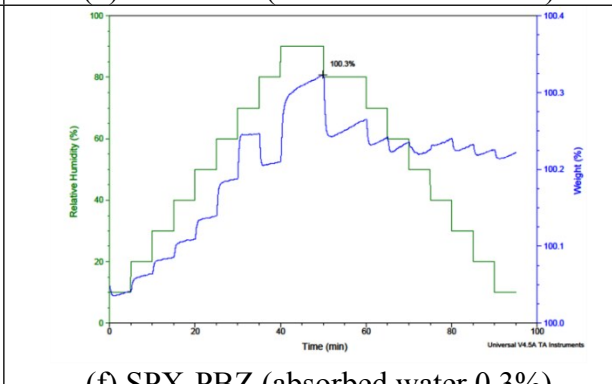

(f) SPX-PBZ (absorbed water 0.3%)

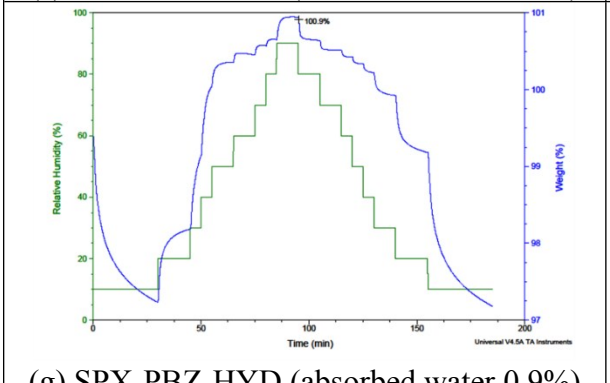

(g) SPX-PBZ-HYD (absorbed water 0.9%)

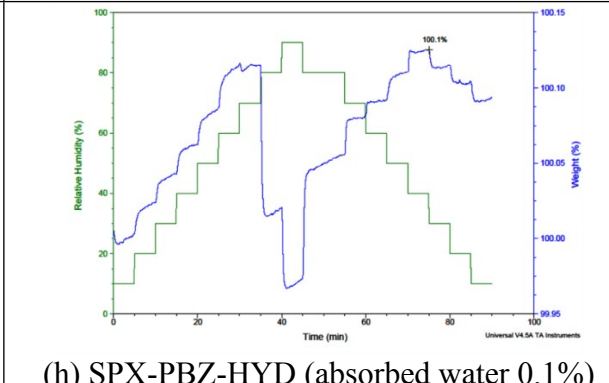

(h) SPX-PBZ-HYD (absorbed water 0.1%)

Experimental Section

SPX-ZW form II (purity >99.8%) was purchased from Yarrow Chem Products (Mumbai, India) and coformers were purchased from Sigma Aldrich (Hyderabad, India). Solvents (purity >99%) were purchased from Hychem Laboratories (Hyderabad, India).

Preparation of Cocrystal

SPX-MBZ: 392.3mg of SPX (0.1mmol, >99.8% purity) and 153mg (0.1mmol, >99.8% purity) of MBZ were co-grinded with acetonitrile solvent.The formation of cocrystal was confirmed by PXRD, DSC and FT-IR.30mg of this material was dissolved in 5 mL chloroform and left for slow evaporation at ambient conditions. Single crystals suitable for X-ray diffraction were obtained after 2-3 days.

SPX-EBZ: 392.3mg of SPX (0.1mmol, >99.8% purity) and 166mg (0.1mmol, >99.8% purity) of EBZ were co-grinded with acetonitrile solvent.The formation of cocrystal was confirmed by PXRD, DSC and FT-IR.30mg of this material was dissolved in 5 mL toluene and left for slow evaporation at ambient conditions. Single crystals suitable for X-ray diffraction were obtained after 7 days.

SPX-PBZ: 392.3mg of SPX (0.1mmol, >99.8% purity) and 180mg (0.1mmol, >99.8% purity) of MBZ were co-grinded with acetonitrile solvent.The formation of cocrystal was confirmed by PXRD, DSC and FT-IR.30mg of this material was dissolved in 5 mL 2-propanol and left for slow evaporation at ambient conditions. Single crystals suitable for X-ray diffraction were obtained after 3-4 days.

SPX-IBZ: 392.3mg of SPX (0.1mmol, >99.8% purity) and 194mg (0.1mmol, >99.8% purity) of MBZ were co-grinded with acetonitrile solvent.The formation of cocrystal was confirmed by PXRD, DSC and FT-IR.

SPX-EBZ-HYD: 392.3mg of SPX (0.1mmol, >99.8% purity) and 166mg (0.1mmol, >99.8% purity) of EBZ are co grinded with acetonitrile solvent.The formation of cocrystal was confirmed by PXRD, DSC and FT-IR.

SPX-PBZ-HYD: 392.3mg of SPX (0.1mmol, >99.8% purity) and 180mg (0.1mmol, >99.8% purity) of MBZ were co-grinded with acetonitrile solvent.The formation of cocrystal was confirmed by PXRD, DSC and FT-IR.

Powder X-ray diffraction

Powder X-ray diffraction was recorded on Bruker D8 Advance diffractometer (Bruker-AXS, Karlsruhe, Germany) using Cu-Kα X-radiation (λ = 1.5406 Å) at 40 kV and 30 mA power. X-ray diffraction patterns were collected over the 2θ range 3–50° at a scan rate of 3.9°/min. Powder Cell 2.4(Federal Institute of Materials Research and Testing, Berlin, Germany) was used for Rietveld refinement of experimental PXRD and calculated lines from the X-ray crystal structure.

Vibrational spectroscopy

Thermo-Nicolet 6700 FT-IR-NIR spectrometer with NXR FT-Raman module (Thermo Scientific, Waltham, MA) was used to record IR spectra. IR spectra were recorded on

samples dispersed in KBr pellets. Data were analysed using Omnic software (Thermo Scientific, Waltham, MA).

Thermal analysis

Differential scanning calorimetry was performed on Mettler-Toledo DSC 822e module, (Mettler-Toledo, Columbus, OH). Samples were placed in crimped but vented aluminium pans for DSC experiments. The typical sample size is 3-5 mg for DSC. The temperature range for the heating curves was 30-350°C, and the sample was heated at a rate of 10 °C/ min. Samples were purged in a stream of dry nitrogen flowing at 80 mL/min.

X-ray crystallography

X-ray reflections were collected on Oxford CCD X-ray diffractometer (Yarnton, Oxford, UK) equipped with Mo-Kα radiation (λ = 0.71073 Å) and Cu-Kα X-radiation (λ = 1.5406 Å) source and data reduction was performed using CrysAlisPro 171.33.55 software.Crystal structures were solved and refined using Olex2-1.0 with anisotropic displacement parameters for non-H atoms.BrukerD8 QUEST CCD diffractometer. Mo-Kα (λ = 0.71073 Å) radiation was used to collect X-ray reflections on all crystals.Bruker D8 Quest diffractometer equipped with a graphite mono chromator and Mo-Kα fine-focus sealed tube (λ = 0.71073 Å). Intensities for absorption were corrected using SADABS. Structures were solved and refined using SHELXL-97 with anisotropic displacement parameters for non-H atoms. Hydrogen atoms on O and N were experimentally located in all crystal structures.Hydrogen atoms were experimentally located through the Fourier difference electron density maps in all crystal structures. All O–H and C–H atoms were geometrically fixed using HFIX command in SHELX-TL program of Bruker-AXS. Crystal parameters (Table S2) and Hydrogen bond distances shown in Table S3 are neutron normalized to fix the D–H distance to its accurate neutron value in the X-ray crystal structures (O–H 0.983 Å, N–H 1.009 Å, and C–H 1.083 Å). X-Seed was used to prepare packing diagrams. Crystallographic .ciffiles are available at www.ccdc.cam.ac.uk/data or as part of the Supporting Information.

Solid-state NMR spectroscopy

Solid-state ^{13}C NMR spectra were recorded on BrukerAvance 400 MHz spectrometer (Bruker- Biospin, Karlsruhe, Germany). ss-NMR measurements were carried out on Bruker 4-mm double resonance CP-MAS probe in zirconia rotors with a Kel-F cap at 5.0-kHz spinning rate with a cross-polarization contact time of 2.5 ms and a delay of 8 s. ^{13}C NMR spectra were recorded at 100 MHz and referenced to the methylene carbon of glycine, and then recalibrated to the TMS scale ($\delta_{glycine}$ = 43.3 ppm).

Solubility measurements

Solubility of SPX and its cocrystals in pH 7 phosphate buffer medium was determined by using intrinsic dissolution rate and equilibrium solubility method. The known concentrations of solutions of were prepared in pH 7 phosphate buffer into 100mL volumetric flask to dissolve the compound and after complete dissolution the flask was to the mark with pH 7 phosphate buffer medium. First, the absorbance of a known concentration of the SPX and its cocrystals was measured at the given λ_{max}(SPX 365 nm) in purified pH 7 phosphate buffer medium on Thermo Scientific Evolution 300 UV-vis spectrometer (Thermo Scientific, Waltham, MA). These absorbance values were plotted against several known concentrations to prepare the concentration vs. intensity calibration curve. From the slope of the calibration curves, molar extinction coefficients for SPX and its cocrystals were calculated. Intrinsic dissolution rate (IDR) of SPX and its cocrystals were carried out on aUSPcertifiedElectrolab TDT-08 L Dissolution Tester (Electrolab, Mumbai, MH, India). In intrinsic attachment unit

250 mg sample (SPX/cocrystals)is compressed between the smooth surfaces under the pressure of 2.5 ton/inch^2 for 4 minan area of 0.5 cm^2. Then the pellets were dipped into 500ml of pH7.0 phosphate buffer medium at 37°C at rotating paddle of 150 rpm.A 5ml of dissolution medium was collected at an interval of 10 min for first six samples and 30 min for next six readings by replacing each with same amount of fresh pH7.0 phosphate buffer. The absorbance is plotted against time for samples collected at regular intervals for SPX and cocrystals were calculated. A 150mg of the sample (SPX/its cocrystal) was added to 5 mL of purified water/ pH 7 phosphate buffer medium. The supersaturated solution was stirred at 600 rpm using a magnetic stirrer at 30 °C. After 24 h, the suspension was filtered through Whatmann 0.45µm syringe filter. Then equilibrium solubility is calculated as per procedure and remaining residues of SPX and its salts were characterized by PXRD

Dynamic Vapor Sorption (DVS) analysis

DVS measurements were performed using a Q5000SA vapor sorption analyzer (TA Instruments, Delaware, and USA) at 40 °C. About 3-5 mg of the sample was placed in a metallic quartz sample pan and subjected to relative humidity flux from 10% to 90% and back to 10% RH with a step size of 10% change in humidity. A dwell time of 60 min was set for a weight change of >0.1% in the adsorption/desorption phase at a particular RH (5 min dwell time for a weight change of <0.1%). Thus, if the weight loss/gain is >0.1% at a particular RH, the instrument maintains the same RH for 60 min and then automatically sets at the next higher/lower value. If the weight gain/loss is <0.1%, the DVS cycle (10–90–10%) will be completed within 90 minutes, otherwise it will take a longer duration